ELECTRONIC SUPPLEMENTARY INFORMATION (ESI)

Bz-8HQ: A Novel Supramolecular Fluorochrome Exhibiting Multiple Stimuli Responsiveness

Lamia A. Siddig[a], Rukayat Bojesomo[a], Mohammad A Khasawneh[a], Abdelouahid Samadi[a], Alejandro Perez Paz[a]*, Haythem A. Saadeh[a,b]*, Na'il Saleh[a]*

[a]Department of Chemistry, College of Science, United Arab Emirates University, P.O. Box 15551, Al Ain, United Arab Emirates

[b]Department of Chemistry, School of Science, The University of Jordan, Amman 11942, Jordan

INDEX OF CONTENTS

Part I: Synthesis of Bz-8HQ Chromophore

Reagents and sample preparation

CB7 and CAD (purity>99.9%) were purchased from Sigma-Aldrich and used as received without further purification. CB7 was assumed to contain 20 % water as notified by the supplier. Millipore water was used with electrical conductivity less than 0.05 μS.

Instruments

^{1}H-NMR and ^{13}C-NMR spectra in D_2O with reference in ppm to a TMS standard were recorded using a Varian-400 MHz (USA) machine at room temperature. Melting points were determined in open capillary tube on a Sanyo Gallenkamp MPD 350-BM 3.5. FT-IR spectra were recorded in a Thermo Nicolet Nexus 470 FT-IR spectrophotometer (USA). The UV-vis spectra were measured in a Cary-300 instrument (Varian) and Hellma absorption cuvettes (path length = 10 mm, volume = 3.5 mL) were used in absorbance measurements. Fluorescence spectra in solution were recorded on a Cary-Eclipse instrument. The slit widths were 2 nm and 2 nm for both the excitation monochromator and emission monochromator in all experiments.

Synthesis of tert-butyl 4-(1H-benzo[d]imidazol-2-yl)piperazine-1-carboxylate 3

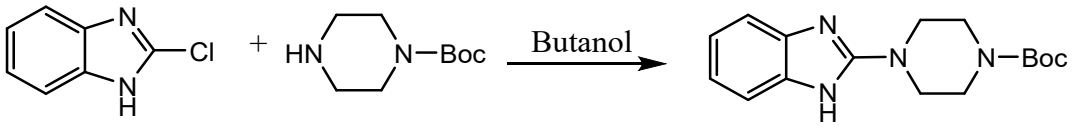

1 **2** **3**

A mixture of 2-chlorobenzimidazole **1** (3.0 g, 19.6 mmol) and N-tert-butoxycarbonyl piperazine **2** (3.7 g, 20 mmol) in 1-butanol (40 mL) was heated to reflux overnight. After finishing, the precipitate was collected and rinsed with ether and dried over high vacuum to obtain tert-butyl 4-(1H-benzimidazol-2-yl)piperazine-1-carboxylate[1] **3** with the following characteristics: white solid, (m = 5.603g, 94.5%); mp 317-319 °C; R_f = 0.8 (1:1 Ethyl acetate/

Hexane); IR (KBr, cm^{-1}) 1650 (C=O), 3407(NH); ^{1}H-NMR (400 MHz, $CDCl_3$) δ 7.49 (dd, J = 5.9, 3.2 Hz, 2H), 7.15 (dd, J = 5.9, 3.2 Hz, 2H), 4.04 – 3.83 (m, 4H), 3.74 – 3.53 (m, 4H), 1.45 (s, 9H); ^{13}C-NMR (101 MHz, $CDCl_3$).

Synthesis of 2-(piperazin-1-yl)-1*H*-benzo[d]imidazole 4

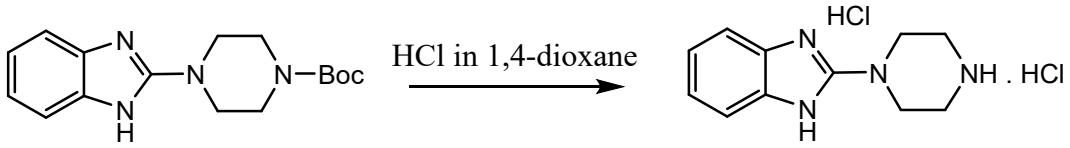

3 **4**

A mixture of N-Boc protected amine **3** (5.3 g, 1 equiv.) in dioxane (10 mL) was added to 4 M of HCl in dioxane (106 mL). The reaction mixture was stirred at room temperature for 3 h. After completion of the reaction, the precipitate was filtered and dried under high vacuum to obtain 2-(piperazin-1-yl)-1H-benzimidazole **4** in quantitative yield[1,2]. White solid, (m = 4.82g, 96%); mp 317-319 °C; R_f = 0.25 (Ethyl acetate), IR (KBr, cm^{-1}) 3380 (NH); ^{1}H-NMR (400 MHz, CD_3OD) δ: 7.50 – 7.41 (m, 2H), 7.38 – 7.32 (m, 2H), 4.01 – 3.91 (m, 4H, 4x Pip-H), 3.55 – 3.46 (m, 4H, 4x Pip-H). ^{13}C-NMR (101 MHz, CD_3OD) δ 149.91, 129.72, 124.11, 111.38, 43.25, 41.92.

Synthesis of 5-chloromethyl-8-quinolinol hydrochloride 6

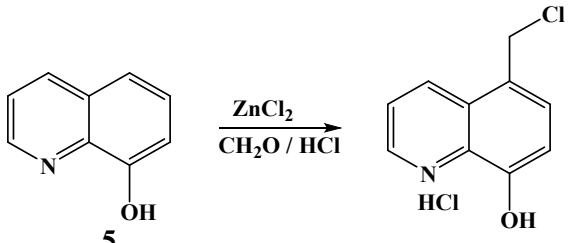

5 **6**

A mixture of 8-hydroxyquine **5** (5.84 g, 70.0 mmol), with zinc chloride (1.05 g, 29.6 mmol) in 50 ml of concentrated hydrochloric acid, and 6.4 ml of 37% formaldehyde was stirred overnight.

The mixture was filtered, washed with acetone and dried to obtain the desired compound **6**. The yellow solid obtained (7.94 g, 86%). ^{1}H-NMR (400 MHz, Deuterium Oxide) δ 9.06 (dd, J = 8.7, 1.4 Hz, 1H), 8.81 (dd, J = 5.4, 1.4 Hz, 1H), 7.90 (dd, J = 8.7, 5.4 Hz, 1H), 7.53 (d, J = 8.0 Hz, 1H), 7.18 (d, J = 8.0 Hz, 1H), 4.87 (d, J = 0.6 Hz, 2H). ^{13}C-NMR (101 MHz, D_2O) δ 145.96, 143.02, 141.86, 129.99, 127.84, 127.36, 127.15, 121.70, 115.05, 59.77.

Synthesis of the Bz-8HQ Chromophore

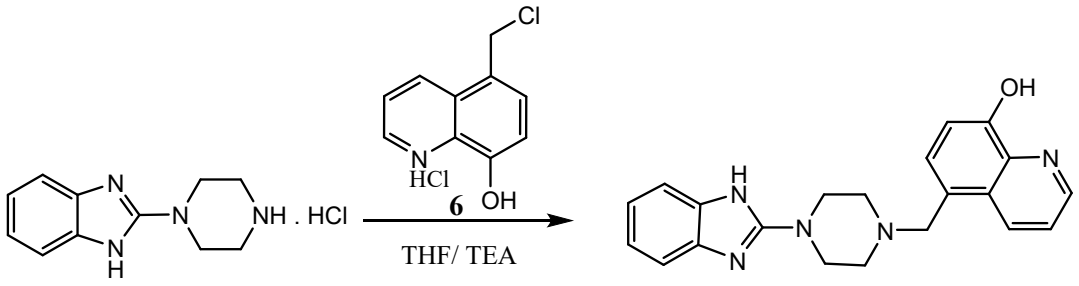

4 **Bz-8HQ**

To a stirred solution of 2-(piperazin-1-yl)-1H-benzo[d]imidazole **4** (0.5 mmol) in tetrahydrofuran (10 mL), triethylamine (460 μL, 4 mmol) was added 5-chloromethyl-8-quinolinol hydrochloride **6** (0.5 mmol). The mixture was stirred at room temperature overnight. After completion, the solvent was removed under vacuum, dissolved in ethyl acetate (20 mL) then washed with water. The organic layer was dried over anhydrous sodium sulfate, the solvent was evaporated, the crude was crystalized over ethyl acetate and the precipitate formed was filtered and dried to obtain the desired compounds. White solid, (0.115 g, 63%); mp 276-278 ^{o}C; R_f = 0.44 (Ethyl acetate) IR (KBr, cm^{-1}) 3077(NH), 3326 (OH); ^{1}H-NMR (400 MHz, DMSO-d_6) δ 11.34 (s, 1H), 9.76 (s, 1H), 8.86 (dd, *J* = 4.1, 1.6 Hz, 1H), 8.69 (dd, *J* = 8.6, 1.7 Hz, 1H), 7.60 (dd, *J* = 8.6, 4.1 Hz, 1H), 7.37 (d, *J* = 7.8 Hz, 1H), 7.16 (dd, *J* = 18.9, 7.6 Hz, 2H), 7.01 (d, *J* = 7.7 Hz, 1H), 6.97 – 6.84 (m, 2H), 3.83 (s, 2H), 3.43 (t, *J* = 5.0 Hz, 4H), 2.53 (d, J = 4.3 Hz, 4H). ^{13}C-NMR (101 MHz, DMSO) δ 156.49, 153.41, 148.24, 139.32, 134.27, 129.52, 128.34, 124.21,

121.93, 110.43, 60.04, 52.36, 46.47. HRMS (ESI): m/z calculated for $C_{21}H_{22}N_5O$ $[M+H]^+$ 360.18244, found 360.18189.

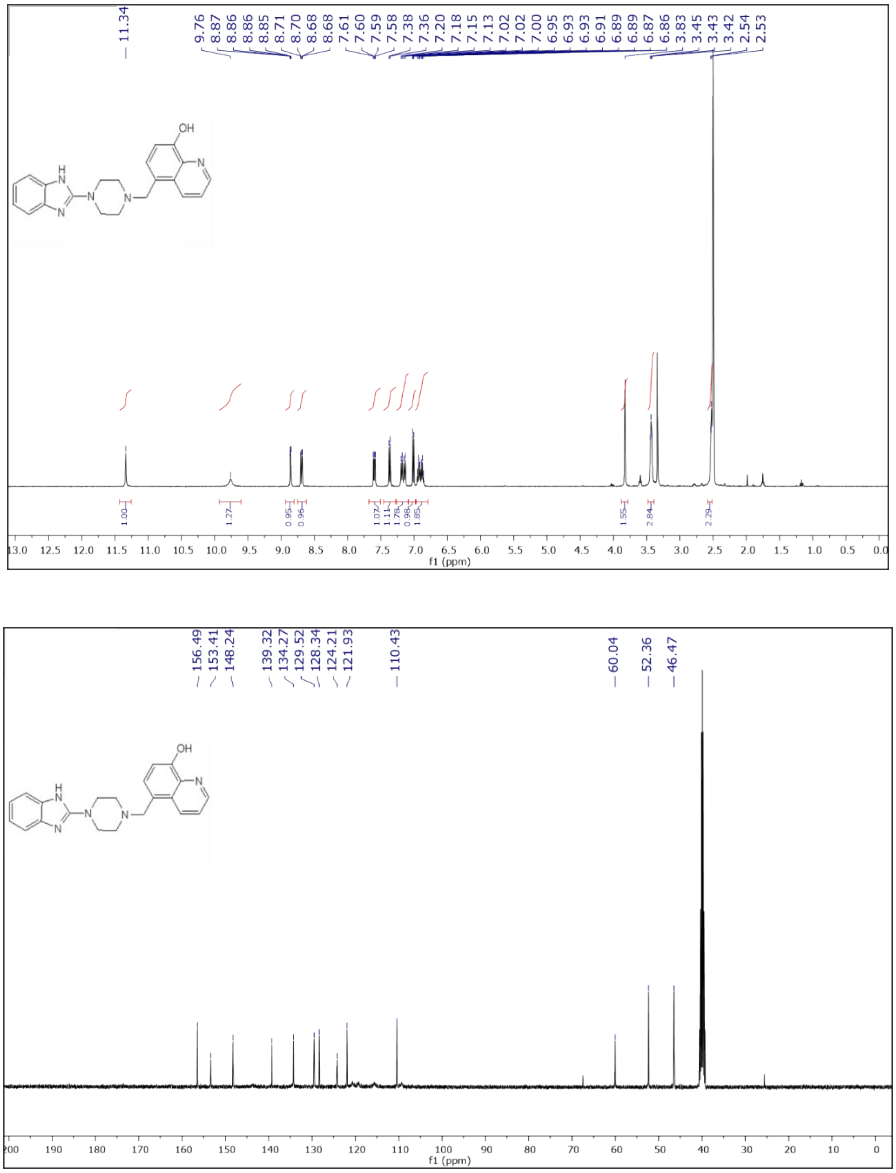

Figure S1. ^{1}H (Top) and ^{13}C (Bottom) NMR spectra for Bz-8HQ chromophore in DMSO-d_6

Part II: Binding experiment of Bz-8HQ with CB7, CAD and HCl

NMR titration experiments of Bz-8HQ.

In NMR titration experiment, the pH values of the solutions were adjusted by adding deuterated HCl (DCl) and recorded using a pH-meter (WTW 330i equipped with a WTW SenTix Mic glass electrode). For the NMR titration experiments of compound Bz-8HQ with CB7, the pD of D_2O was adjusted to 2.9 in which a stock solution of Bz-8HQ was prepared with a final concentration of ~2 mM. Then, a calculated weight of CB7 (0.2 equivalent) was added to compound Bz-8HQ solution in the NMR tube. The 0.2 equivalents of CB7 were gradually added to the solution to complete the titration. The NMR spectra were measured for each solution[3].

For the titration experiment of the Bz-8HQ/CB7 complex with CAD at pH 1.3, a stock solution of Bz-8HQ [2 mM] and CB7 [4 mM] complex was prepared. Then, a calculated weight of CAD (0.5 equivalent) was added to the complex in the NMR tube. In the titration of CAD with CB7 at pH 4.6, a stock solution of CAD [2 mM] was prepared, and then a calculated weight of CB7 (0−1.2 equiv.) was added gradually to the solution. In the titration of CAD with Bz-8HQ at pH 4.6, calculated weight of Bz-8HQ (0−0.7 equiv.) was added gradually to the stock solution of CAD [2 mM].

The effects of adding HCl, CB7 and CAD on UV-Visible absorption properties of Bz-8HQ.

In the titration experiment, the concentrations of the guest were kept constant and the host (CB7) was gradually increased. The spectra were plotted as a function of the CB7 concentrations at a given wavelength. The stock solutions were (i) Bz-8HQ in water [35 μM] with/without [500 μM] CB7, and (ii) CAD in water [500 μM]. In the binding experiment, we added aliquots of solution (ii) to a fixed volume (2.4 mL) of solution (i).

In the binding experiment of compound Bz-8HQ with CB7, the following procedure was adopted: 35 μM of Bz-8HQ solution was placed in cuvette with 1-cm optical path length and

small amounts of the CB7 solution (1 mM) were gradually added with micropipette. For the interaction of the Bz-8HQ/CB7 complex with CAD, 35 µM of Bz-8HQ and 350 µM of CB7 solution were placed in the same cuvette and small amounts of the CAD solution (1 mM) were gradually added with micropipette[1].

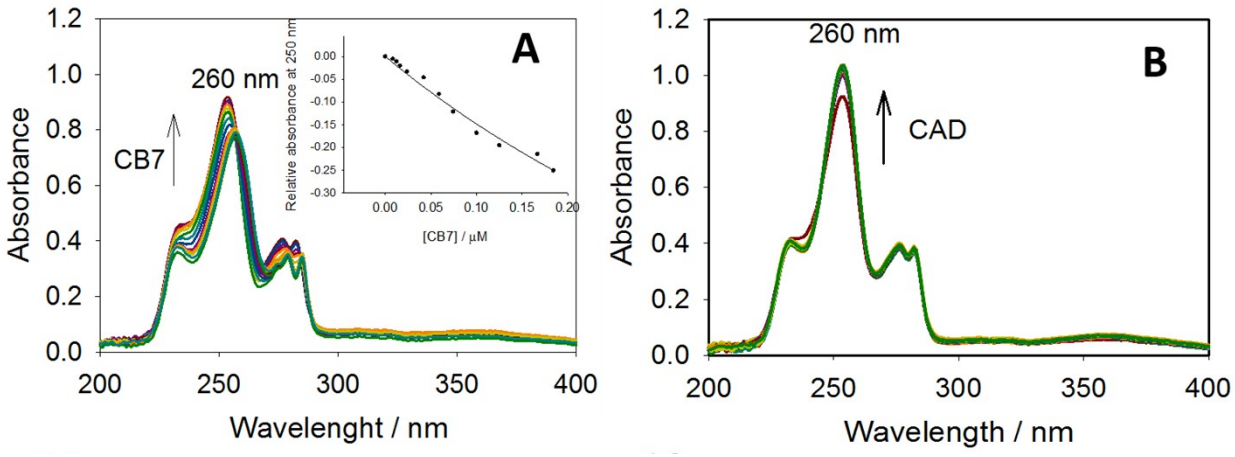

Figure S2. UV−vis absorption spectra at pH 4.6: **A** shows the binding titration of Bz-8HQ with CB7. **B** shows the binding titration of the Bz-8HQ with cadaverine.

Figure S2**A** shows the variation of UV−vis spectra of Bz-8HQ [35 µM] upon the addition of CB7 (0−500 µM). The fluorescent compound (Bz-8HQ) has an absorption around 260 nm. As the concentrations of CB7 increases (0−500 µM), the absorption increases with a slight blue shift, which confirms the encapsulation of Bz-8HQ in CB7. Figure S2**B** shows the UV−vis spectra of binding titration of Bz-8HQ with CAD (0−500 µM) at pH 4.6. The absorption of Bz-8HQ at 260 nm increases and slightly shifts to the left, upon the addition of CAD (0−500 µM).

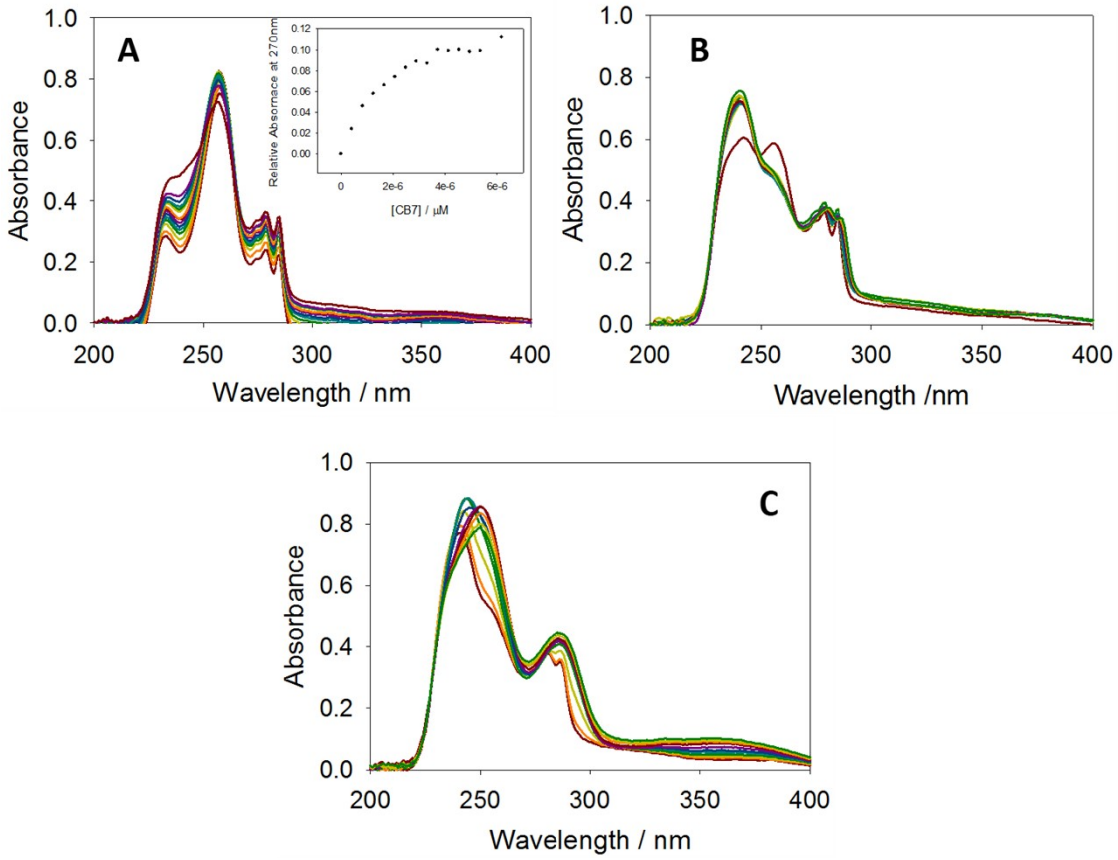

Figure S3. UV−visible absorption: Binding titration of CAD with the complex of Bz-8HQ and CB7 at pH 4.6: **A** (0−30 µl). **B** (34−60 µl). **C** (65−1600 µl).

Figure S3 shows the variation of UV−vis absorption spectra of Bz-8HQ/CB7 complex (32.1 µM for Bz-8HQ and 500 µM for CB7) upon the addition of different volumes of CAD [500 µM] at fixed pH of 4.6. Figure S3**A** illustrates that upon the addition of (0−30 µl) of CAD, the absorption of the complex at 260 nm was not affected, whereas in Fig. S3**B**, the addition of (34−60 µl) of CAD generated a new absorption peak around 240 nm on the expense of the band at 260 nm as evidenced by the formation of an isosbestic point at 250 nm. The change in the absorption profile of Bz bands indicates its replacement from the cavity of CB7 by CAD, in agreement with the NMR data above. Figure S3**C**, on the contrary, confirms the interaction of

CAD with the 8HQ unit upon the addition of (65 −1600 µl) by virtue of the gradual development of a new peak at 250 nm.

Part III: Stimuli emission responsiveness of Bz-8HQ to the addition of HCl, CB7 and CAD.

Operation through PET mechanism (excitation of 8HQ moiety at 375 nm)

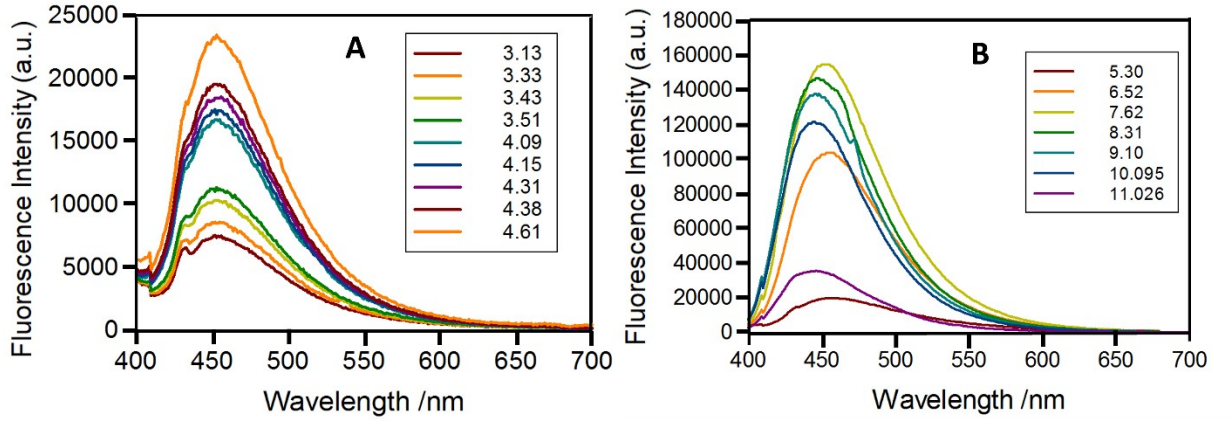

Figure S4. The fluorescence intensity of Bz-8HQ. **A**: in acid media. We observe an increase of peak intensity as pH increases in the series 3.13, 3.33, 3.43, 3.51, 4.09, 4.15, 4.31, 4.38 and 4.61. **B** pH from 5.3 to 11.

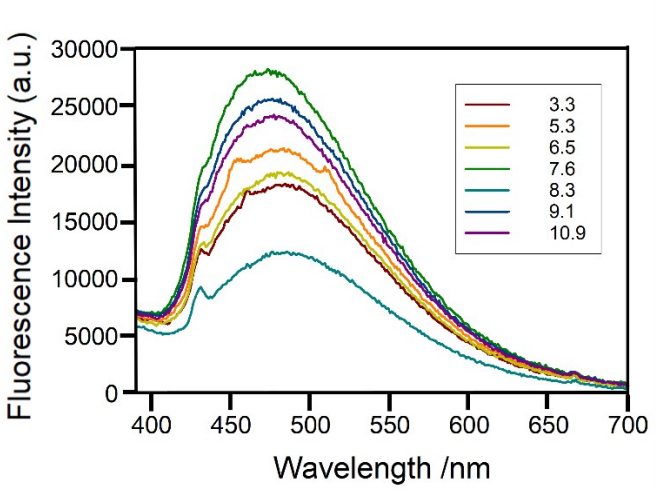

Figure S5. The fluorescence intensity of Bz-8HQ/CB7 complex from pH 3.3 to 10.9. The figure shows the evolution of peak intensities as pH increases in the series 3.3, 5.3, 6.5, 7.6, 8.3, 9.1, and 10.9.

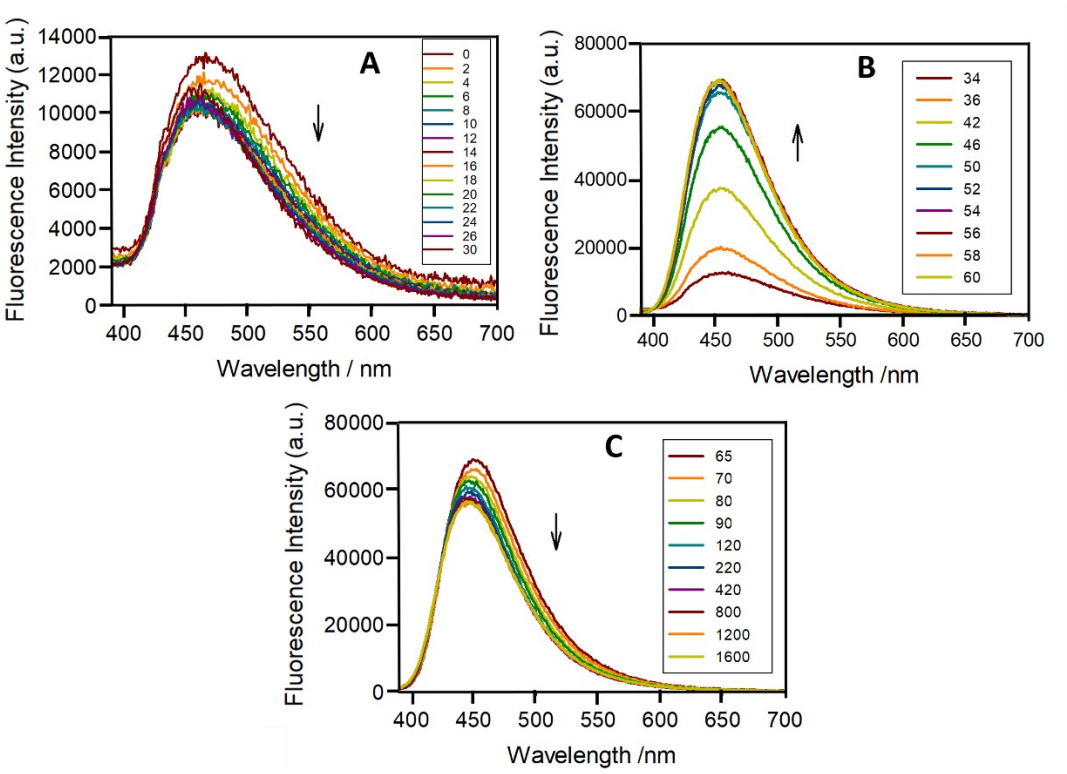

Figure S6. Fluorescence titration of CAD with the complex of Bz-8HQ and CB7 at pH 4.6: **A** (0−30 µl). **B** (34−60 µl). **C** (65−1600 µl). The arrows indicate the time evolution of peak intensity as concentration of CAD increases from 0 to 1600 µl.

Part IV: Computational Details

Ab initio Geometry optimizations

All density functional theory (DFT) calculations were performed using the freely available program ORCA (version 4.2.1).[2] Geometry relaxations of individual molecules used the hybrid exchange-correlation functional B3LYP[3,4] supplemented with van der Waals corrections according to the Grimme's D3 approach[5,6] with the Becke-Johnson damping scheme (D3BJ). For the large CB7-guest complexes, however, we used the BLYP functional instead of the computationally expensive hybrid B3LYP functional. We used a triple-zeta quality basis set (def2-TZVP) from Ahlrichs and coworkers[7] and the "TightSCF" keyword for all geometry relaxations for accurate evaluation of the ionic forces. Calculations that required inclusion of solvent effects were performed using implicit water within the conductor-like polarizable continuum model (CPCM). No imaginary frequencies were found in the vibrational calculations which confirms that all relaxed ground state geometries were true stationary points of the electronic ground state potential energy surface. Visualization and rendering were carried out with the VMD code.[8]

Simulated TDDFT UV-Visible spectra

The optical properties were calculated within the time-dependent density functional theory (TDDFT) approach. For the calculation of absorption spectra and excited-state properties we used two different hybrid functionals: the standard B3LYP and the long-range corrected ωB97X-D3 functional.[6,9,10] A total of 50 singlet roots were computed within the Tamm-Dancoff

approximation (TDA). Additionally, we employed the RIJCOX approximation for the Coulomb integrals to speed up TDDFT calculations with hybrid functionals with minimal impact on the simulated spectra. All optical calculations used the def2-TZVP basis set. We generated the simulated UV-Vis spectra by centering a Gaussian of full width at half maximum (FWHM) of 800 cm^{-1} on each transition.

Force-Field Molecular Dynamics (MD) calculations

Classical molecular dynamics (MD) simulations in explicit water were carried out using the "sander" module of AMBER 20 suite[11].We parametrized the charges of CB7 and ligand molecules at the AM1-BCC semiempirical level[12] using the "antechamber" code. The second-generation of the AMBER force field GAFF2[13] was used in all the calculations. The systems were solvated with 1176 TIP3P[14] water molecules in a truncated octahedral periodic box of about 35.9 Å, which extends about 11 Å from the guest-host complexes. We keep the same number of water molecules (1176) in all of our MD simulations for consistency. Two chloride ions (Cl^-) were randomly placed in the simulation box to keep the overall charge neutrality of the system (CB7 is neutral but both CAD and Bz-8HQ ligands are +2 charged in their bi-protonated state). The non-bonded cutoff was set to 9 Å and the time step was 2 fs, which ensure a good stability in the MD simulations. Prior to the MD runs, the systems were subjected to 10,000 cycles of steepest descent energy minimization to relieve bad steric contacts. This was followed by a constant-pressure (1 bar) equilibration at 298.15 K for over 30 ns. The production runs were performed for over 16 ns in the NPT ensemble. The host-guest binding free energy was estimated from the production MD trajectories using the Generalized Born (GB) model as implemented in the MMPBSA.py code[15]. The binding enthalpies in solution were also estimated

from the mean values of the potential energies over the production MD runs and consistent values were found compared to the MMPBSA.py code.

Part V: Simulated UV-Visible spectra of Bz-8HQ

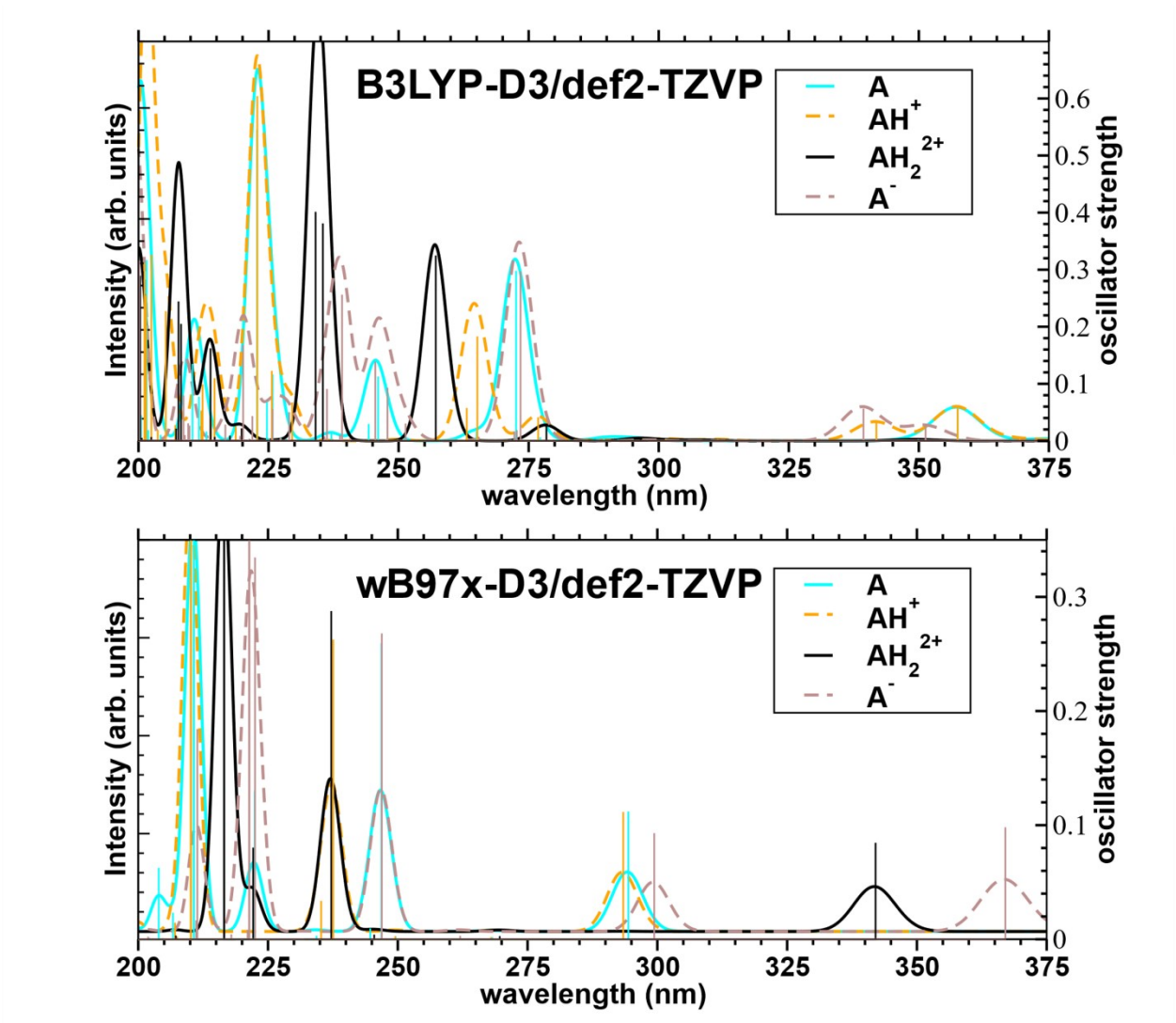

Figure S7. Simulated TDDFT electronic absorption spectra of the protomers of Bz-8HQ ("A" in legend) at the B3LYP-D3 (Top) and ωB97X-D3 (Bottom) levels of theory. Individual electronic transitions are marked by the vertical spikes, with oscillator strengths given on the right vertical axis.

We simulated the UV-Vis absorption spectra of Bz-8HQ and its protonation states using time-dependent density functional theory (TDDFT) at the B3LYP-D3/def2-TZVP level using implicit water, see Figure S4. We also employed hybrid long-range corrected ωB97x-D3 exchange-correlation functional due to the potential charge transfer character of some electronic transitions. Both functionals correctly predict a blue-shift of the lowest energy peak (see experimental peak at 287 nm at pH=8.7 in Fig. 2b) as Bz-8HQ$^-$ anion becomes successively protonated, in agreement with experimental UV-Vis spectra (Fig. 2). Between the two DFT functionals, B3LYP seems to reproduce better the position of the peaks shown in Fig. 2 of the main text.

References

(1) Fukuzumi, S. Nanocarbons as Electron Donors and Acceptors in Photoinduced Electron-Transfer Reactions. *ECS J. Solid State Sci. Technol.* **2017**, *6* (6), 3055–3061. https://doi.org/10.1149/2.0061706jss.

(2) Neese, F. The ORCA Program System. *WIREs Comput. Mol. Sci.* **2012**, *2* (1), 73–78. https://doi.org/https://doi.org/10.1002/wcms.81.

(3) Becke, A. D. Density-Functional Thermochemistry. III. The Role of Exact Exchange. *J. Chem. Phys.* **1993**, *98* (7), 5648–5652. https://doi.org/10.1063/1.464913.

(4) Stephens, P. J.; Devlin, F. J.; Chabalowski, C. F.; Frisch, M. J. Ab Initio Calculation of Vibrational Absorption and Circular Dichroism Spectra Using Density Functional Force Fields. *J. Phys. Chem.* **1994**, *98* (45), 11623–11627. https://doi.org/10.1021/j100096a001.

(5) Grimme, S.; Ehrlich, S.; Goerigk, L. Effect of the Damping Function in Dispersion Corrected Density Functional Theory. *J. Comput. Chem.* **2011**, *32* (7), 1456–1465. https://doi.org/https://doi.org/10.1002/jcc.21759.

(6) Grimme, S.; Antony, J.; Ehrlich, S.; Krieg, H. A Consistent and Accurate Ab Initio Parametrization of Density Functional Dispersion Correction (DFT-D) for the 94 Elements H-Pu. *J. Chem. Phys.* **2010**, *132* (15), 154104. https://doi.org/10.1063/1.3382344.

(7) Weigend, F.; Ahlrichs, R. Balanced Basis Sets of Split Valence, Triple Zeta Valence and Quadruple Zeta Valence Quality for H to Rn: Design and Assessment of Accuracy. *Phys. Chem. Chem. Phys.* **2005**, *7* (18), 3297–3305. https://doi.org/10.1039/B508541A.

(8) Humphrey, W.; Dalke, A.; Schulten, K. VMD: Visual Molecular Dynamics. *J. Mol. Graph.* **1996**, *14* (1), 33–38. https://doi.org/https://doi.org/10.1016/0263-7855(96)00018-5.

(9) Chai, J.-D.; Head-Gordon, M. Long-Range Corrected Hybrid Density Functionals with Damped Atom–Atom Dispersion Corrections. *Phys. Chem. Chem. Phys.* **2008**, *10* (44), 6615–6620. https://doi.org/10.1039/B810189B.

(10) Lin, Y.-S.; Li, G.-D.; Mao, S.-P.; Chai, J.-D. Long-Range Corrected Hybrid Density Functionals with Improved Dispersion Corrections. *J. Chem. Theory Comput.* **2013**, *9* (1), 263–272. https://doi.org/10.1021/ct300715s.

(11) Case, D. A.; Belfon, K.; Ben-Shalom, I. Y.; Brozell, S. R.; Cerutti, D. S.; Cheatham, T. E.; III; Cruzeiro, V. W. D.; Darden, T. A.; Duke, R. E.; Giambasu, G.; Gilson, M. K.; Gohlke, H.; Goetz, A. W.; Harris, R.; Izadi, S.; Izmailov, S. A.; Kasavajhala, K.; Kovalenko, A.; Krasny, R.; Kurtzman, T.; Lee, T. S.; LeGrand, S.; Li, P.; Lin, C.; Liu, J.; Luchko, T.; Luo, R.; Man, V.; Merz, K. M.; Miao, Y.; Mikhailovskii, O.; Monard, G.; Nguyen, H.; Onufriev, A.; Pan, F.; Pantano, S.; Qi, R.; Roe, D. R.; Roitberg, A.; Sagui, C.; Schott-Verdugo, S.; Shen, J.; Simmerling, C. L.; Skrynnikov, N. R.; Smith, J.; Swails, J.; Walker, R. C.; Wang, J.; Wilson, L.; Wolf, R. M.; Wu, X.; Xiong, Y.; Xue, Y.; York, D. M.; Kollman, P. A. *AMBER 2020*; University of California, San Francisco, 2020.

(12) Jakalian, A.; Bush, B. L.; Jack, D. B.; Bayly, C. I. Fast, Efficient Generation of High-Quality Atomic Charges. AM1-BCC Model: I. Method. *J. Comput. Chem.* **2000**, *21* (2), 132–146. https://doi.org/https://doi.org/10.1002/(SICI)1096-987X(20000130)21:2<132::AID-JCC5>3.0.CO;2-P.

(13) Wang, J.; Wolf, R. M.; Caldwell, J. W.; Kollman, P. A.; Case, D. A. Development and Testing of a General Amber Force Field. *J. Comput. Chem.* **2004**, *25* (9), 1157–1174. https://doi.org/10.1002/jcc.20035.

(14) Jorgensen, W.; Chandrasekhar, J.; Madura, J.; Impey, R.; Klein, M. Comparison of Simple Potential Functions for Simulating Liquid Water. *J. Chem. Phys.* **1983**, *79*, 926–935. https://doi.org/10.1063/1.445869.

(15) Miller, B. R.; McGee, T. D.; Swails, J. M.; Homeyer, N.; Gohlke, H.; Roitberg, A. E. MMPBSA.Py: An Efficient Program for End-State Free Energy Calculations. *J. Chem. Theory Comput.* **2012**, *8* (9), 3314–3321. https://doi.org/10.1021/ct300418h.